

TUNGSTEN ISOTOPIC EVOLUTION AND MANTLE EQUILIBRATION IN GRAND TACK SIMULATIONS



Nicholas Zube¹ (nzube@ucsc.edu), F. Nimmo¹, and S. A. Jacobson^{2,3}

¹University of California Santa Cruz, Santa Cruz, CA. ²Bayerisches Geoinstitut, Universität Bayreuth, Bayreuth, Germany. ³Laboratoire Lagrange, Observatoire de la Côte d'Azur, Nice, France.



Introduction

Measurements of the radioisotopic Hf/W system found in meteorites and the Earth can be used to place constraints on the timescales of core formation and accretion [1]. Calculations of the tungsten isotopic evolution of planetesimals in "classical" accretion models have been able to produce physical and isotopic values close to those measured presently on the Earth [1,2]. The classical models' difficulty in reproducing the correct mass for Mars inspired the creation of the Grand Tack scenario [3,4]. In this study we examine whether the Grand Tack simulations are able to reproduce the measured tungsten anomalies in final planets resembling Earth and Mars.

Mantle Equilibration

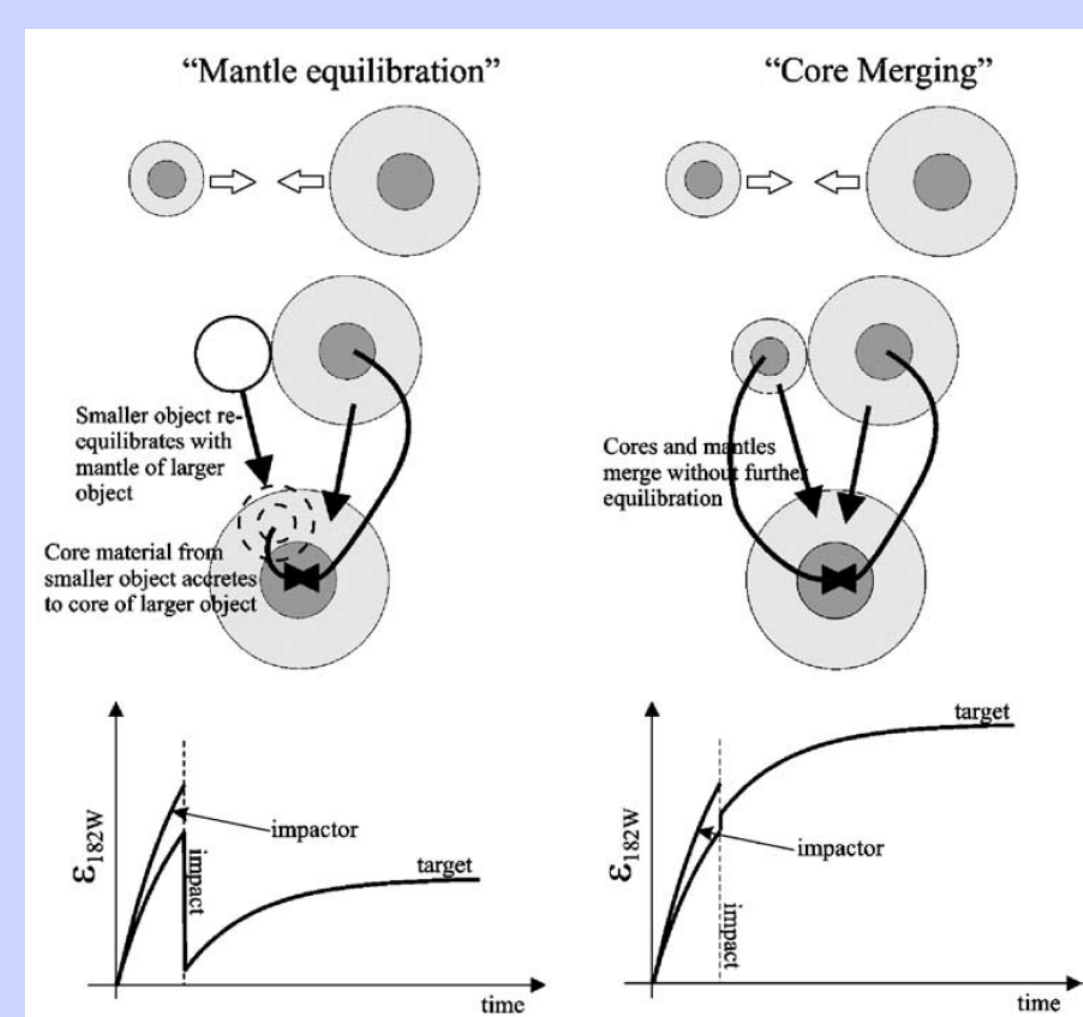


Figure 1: Schematic of the extreme equilibration scenarios represented by $k=1$ (complete mantle re-equilibration) and $k=0$ (core merging) [5]. Generally, we assume the larger body (target) differentiates upon impact if it has not already done so. The lower panels give schematic depictions of the evolution of mantle tungsten anomalies for the target and impactor under the extreme re-equilibration scenarios.

Hf is a lithophile and W a siderophile element, resulting in fractionation during core formation. The decay of ^{182}Hf into ^{182}W with a half life of 9 My causes mantles with early core formation to develop a large positive tungsten anomaly [6]. The tungsten evolution of a mantle depends on how impactor core material re-equilibrates during each individual impact with a target [1,2]. The equilibration factor k is defined as the fraction of impactor core not directly added to target core, where $k=0$ indicates core merging, and $k=1$ indicates complete re-equilibration. For the results in this study, we explored tungsten anomalies produced by a range of k from 0 to 1. Past analyses on the classical accretion scenario found an intermediate value of $k \sim 0.5$ to be most appropriate [1,6].

Isotopic Results

	k	Mantle fractionation	Tungsten anomaly	Accretion Time (My)	N
Earth	-	13.6 ± 4.3	1.9 ± 0.1	-	-
Earth-like (8:1)	0.5	16.6 ± 2.7	6.5 ± 2.9	39 ± 46	26
Earth-like (8:1)	1	17.8 ± 3.0	4.0 ± 2.3	39 ± 46	26
Earth-like (4:1)	0.5	16.5 ± 1.1	6.2 ± 1.9	17 ± 6	18
Earth-like (4:1)	1	18.2 ± 1.2	3.3 ± 1.4	17 ± 6	18
Mars	-	2.4 ± 0.9	2.3 ± 0.2	-	-
Mars-like (8:1)	0.5	11.6 ± 6.3	10.8 ± 5.9	4 ± 7	18
Mars-like (8:1)	1	12.5 ± 6.9	8.5 ± 4.8	4 ± 7	18
Mars-like (4:1)	0.5	7.2 ± 6.3	4.6 ± 3.2	15 ± 28	10
Mars-like (4:1)	1	7.9 ± 7.4	3.4 ± 2.2	15 ± 28	10

Table 1: Summary of results. Mean and standard deviation for final values of bodies are displayed for objects that meet Earth-like or Mars-like criteria (mass within a factor of 2 of present values, Earth-like semi-major axis between present Mercury and Mars values, Mars-like semi-major axis between 1 and 2.3 AU). Measured Earth and Mars are values from [7], [8], [9]. Accretion time refers to the time when the body reached 90% of final mass.

Summary

- The evolution of the Hf/W isotopic system is followed through the accretionary collisions of 28 N-body simulations using the Grand Tack scenario, during which the target cores are assumed to experience partial mantle re-equilibration.
- We find the simulations are able to reasonably reproduce the measured tungsten isotope values for resulting Earth and Mars-sized bodies at an equilibration factor, $k \geq 0.5$, with $k = 1$ providing the highest likelihood of Earth-like outcomes.

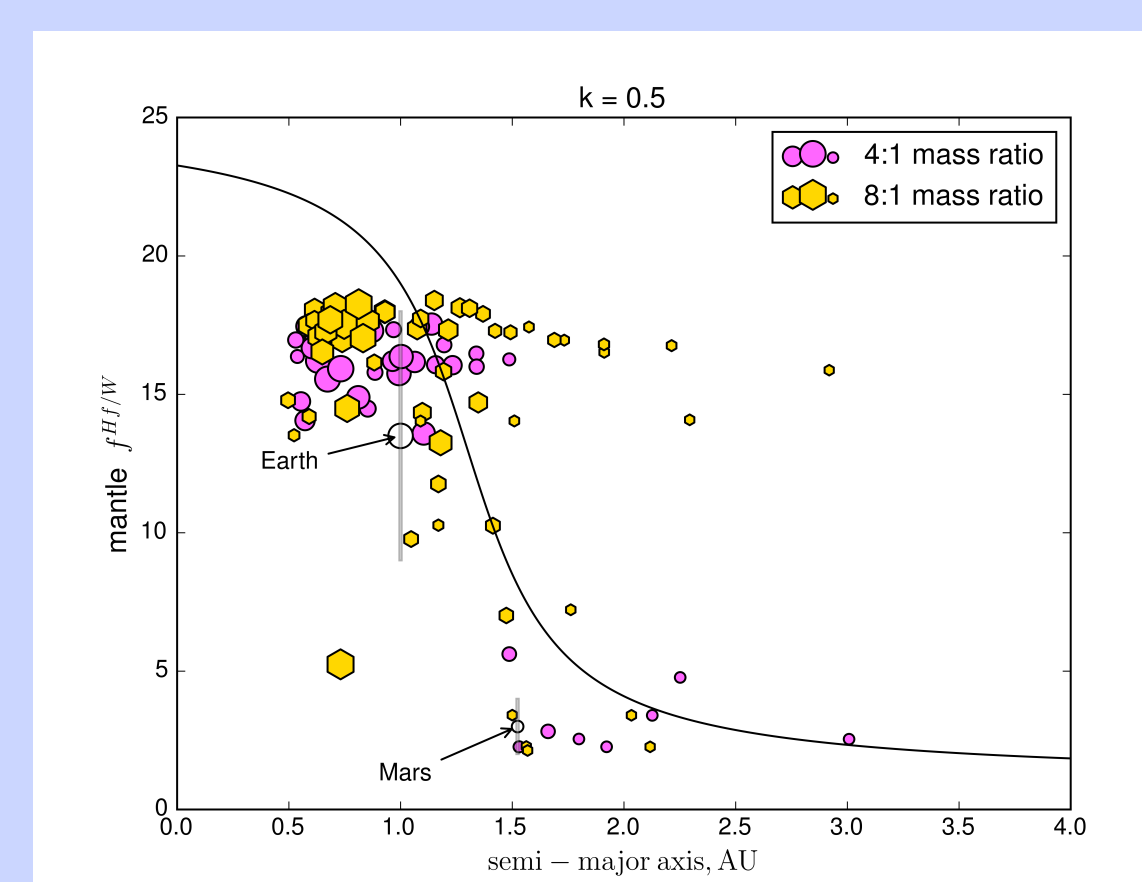


Figure 2: Mantle fractionation factor of surviving bodies as a function of final semi-major axis, for 28 Grand Tack simulations [3]. The solid line denotes initial assumed variation in $f_{\text{Hf/W}}$ [6]. Mass ratio refers to the distribution of initial mass in Mars-sized embryos vs. smaller planetesimals. The size of the markers are scaled to the object's final mass.

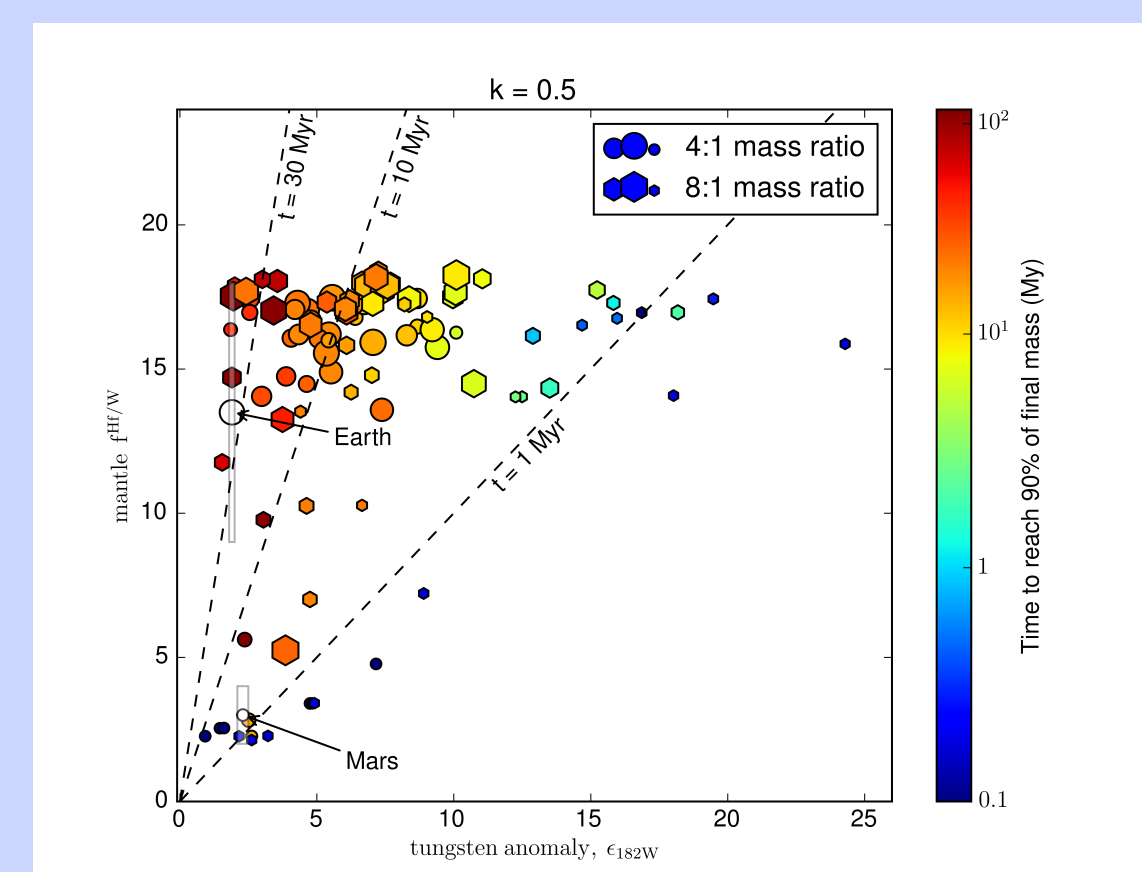


Figure 3: Mantle fractionation factor of surviving bodies as a function of tungsten anomaly. Color scale shows approximate time of last giant impact (or when 90% of final mass was attained). Earth and Mars values (shergottite source, [7]) are plotted as rectangles, with circles also shown for mass comparison.

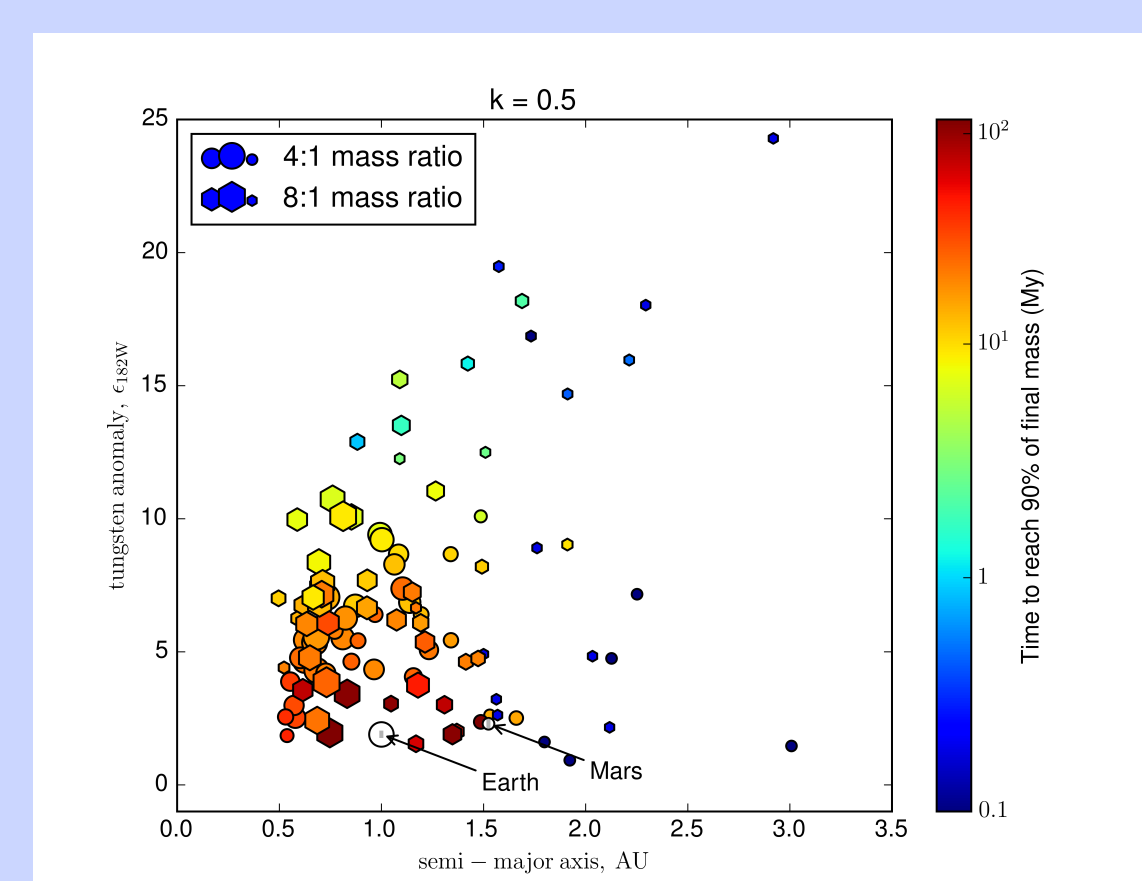


Figure 4: Tungsten anomaly of surviving bodies as a function of final semi-major axis. Color and size are formatted as in Fig. 2. The uncertainties of tungsten anomaly for Earth and Mars are smaller than the circle markers.

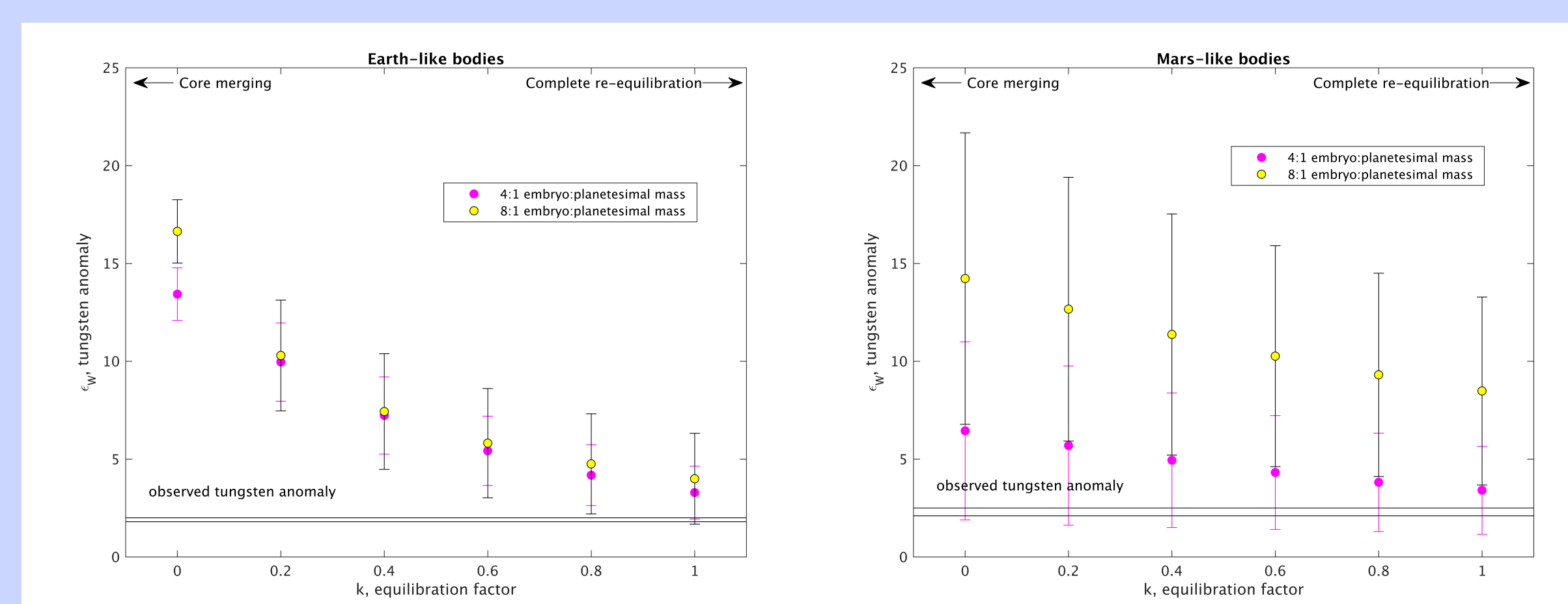


Figure 5: Average tungsten anomaly for bodies meeting Earth-like and Mars-like criteria over a range of values for k . Error bars represent standard deviation. Selection criteria for bodies are described in Table 1.

Results

Fig. 2 shows the mantle fractionation factor as a function of semi-major axis, with the solid line representing the initial assumed values (from [6]). An initial variation in $f_{\text{Hf/W}}$ is one way of explaining the different values measured for Earth and Mars. The initial variation is not completely destroyed, despite the significant radial mixing caused by Jupiter's inwards-then-outwards migration. Lower embryo to planetesimal initial mass distributions may increase dynamical friction in the disk and reduce scattering from initial positions.

In Fig. 3, the variation in mantle fractionation $f_{\text{Hf/W}}$ against tungsten anomaly ϵ_W is shown. Tungsten anomaly increases with increased $f_{\text{Hf/W}}$ but decreases with longer accretion timescales, as expected. Although most model Earth-mass bodies develop large ϵ_W values, because of their rapid accretion, some take longer to complete accretion and produce Earth-like values. Mars analogues accrete rapidly but can develop Mars-like ϵ_W values because of lower $f_{\text{Hf/W}}$ values. Smaller values of k (less equilibration) result in isotopic anomalies which are too large.

In Fig. 4, tungsten anomaly ϵ_W is plotted against semi-major axis. Accretion terminates earlier at larger semi-major axes, but the resulting tungsten anomalies of these outer bodies are highly variable, because of the varying $f_{\text{Hf/W}}$ values. The actual tungsten anomalies for both Earth and Mars sit at the lower end of the envelope of model values, suggesting that $k=0.5$ represents the minimum amount of re-equilibration required (see Fig. 5).

In Fig. 5, average tungsten anomaly of Earth-like and Mars-like planets is plotted over a range of values for k . Values closer to $k=1$ are the best at reproducing measured values for both Earth and Mars. The Grand Tack constructs planets more quickly than the classical models, which causes larger W anomalies, requiring higher k to reproduce measured results.

Discussion

Our study suggests that the Grand Tack scenario is able to construct an Earth and Mars that have both physical and isotopic characteristics in reasonable agreement with measured values, assuming that there is a spatial variation in $f_{\text{Hf/W}}$ and that mantle re-equilibration occurs with a factor of $k \geq 0.5$. Future work should focus on exploring different prescriptions for k , which is likely to depend on the details of individual impacts [10], and on more sophisticated treatments of how $f_{\text{Hf/W}}$ is likely to vary (for instance, as a function of the oxidation state of the starting material [11]).

References

- [1] Kleine T. et al. (2009) *Geochimica et Cosmochimica Acta*, 73, 5150-5188. [2] Rudge J. F., Kleine T. and Bourdon B. (2010). *Nature Geosci.* 3, 439-443. [3] Walsh K. J. et al. (2011) *Nature*, 475, 206-209. [4] Jacobson S. A. and Morbidelli A. (2014) *Phil. Trans. of the Royal Society*, v. 372, iss. 2024. [5] Nimmo F. and Agnor C. B. (2006) *Earth & Planet. Sci. Letters*, 243, 26-43. [6] Nimmo F. et al. (2010) *Earth & Planet. Sci. Letters*, 292, 363-370. [7] Kleine T. et al. (2004) *Geochimica et Cosmochimica Acta*, 68, 2935-2946. [8] Nimmo F. and Kleine T. (2007) *Icarus*, 191, iss. 2, 497-504. [9] Foley C. N. et al. (2005) *Geochimica et Cosmochimica Acta*, 69, 4557-4571. [10] Deguen R., Landeau M., and Olson P. (2014) *Earth & Planet. Sci. Letters*, 391, 274-287. [11] Rubie D. C. et al. (2015) *Icarus*, 248, 89-108.